

Electronic Supplementary Information

Ultrathin Nickel Boride Nanosheets Anchored on Functionalized Carbon Nanotubes as Bifunctional Electrocatalysts for Overall Water Splitting

Xuncai Chen,^a Zixun Yu,^a Li Wei,^a Zheng Zhou,^a Shengli Zhai,^a Junsheng Chen,^a Yanqing Wang,^b Qianwei Huang,^c H. Enis Karahan,^{a, d} Xiaozhou Liao,^c and Yuan Chen^{a,*}

^a The University of Sydney, School of Chemical and Biomolecular Engineering, Sydney, New South Wales, 2006, Australia

^b Faculty of Engineering, The University of Tokyo, Bunkyo-ku, Tokyo 113-0032, Japan

^c The University of Sydney, School of Aerospace, Mechanical and Mechatronic Engineering, Sydney, New South Wales, 2006, Australia

^d School of Chemical and Biomedical Engineering, Nanyang Technological University, 62 Nanyang Drive, Singapore 637459, Singapore

E-mail address: yuan.chen@sydney.edu.au (Y. Chen)

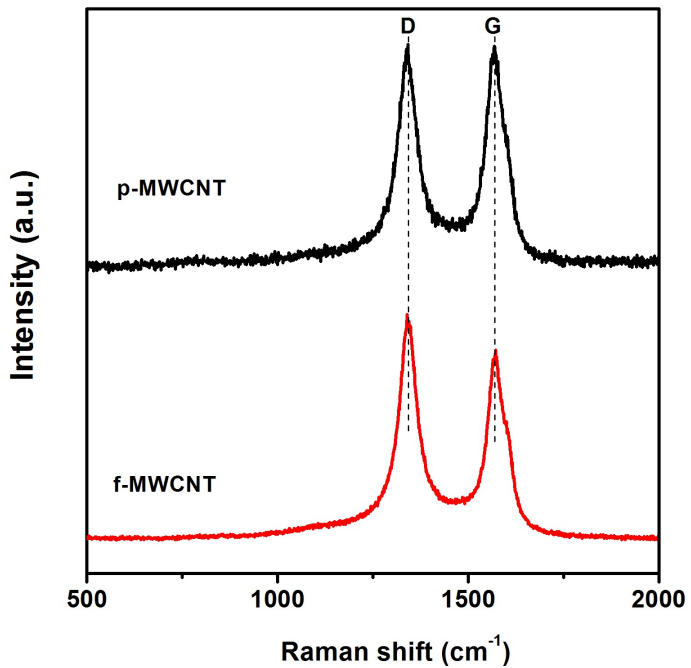


Fig. S1 Raman spectra of commercial multi-walled carbon nanotubes (MWCNTs) at pristine and chemically functionalized forms: p-MWCNTs and f-MWCNTs. (Note that pristine MWCNTs were not subjected to chemical cleaning and tested in their as-received form.)

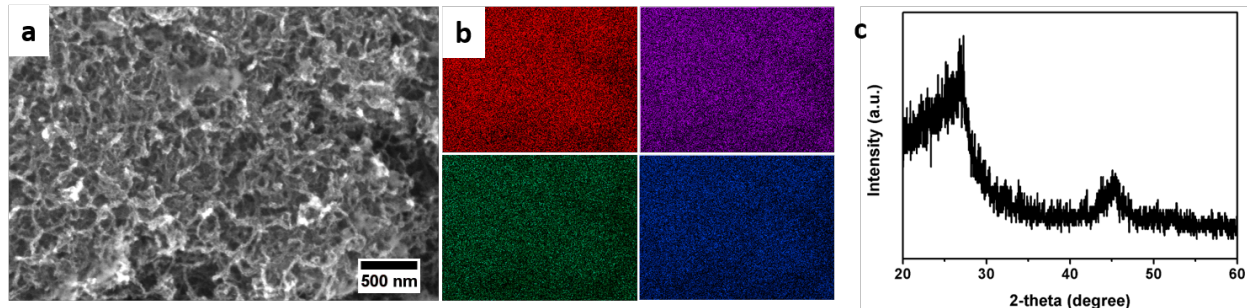


Fig. S2 Characterization of the morphology and structure properties of NixB/f-MWCNT hybrids before 300 °C calcination. (a) SEM; (b) the corresponding EDX elemental mappings of the whole region of (a); (c) XRD.

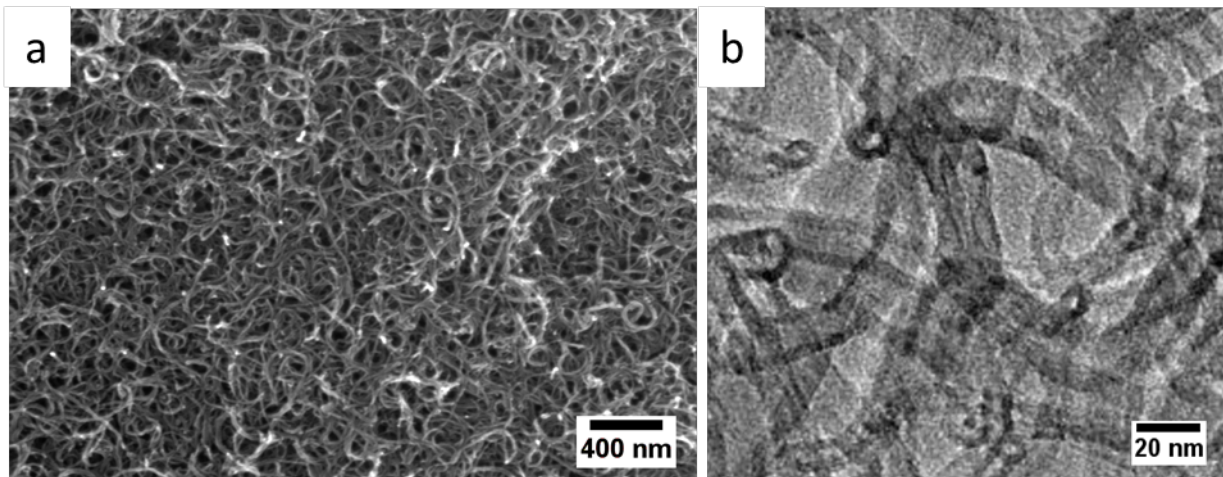


Fig. S3 (a) SEM and (b) TEM images of f-MWCNTs.

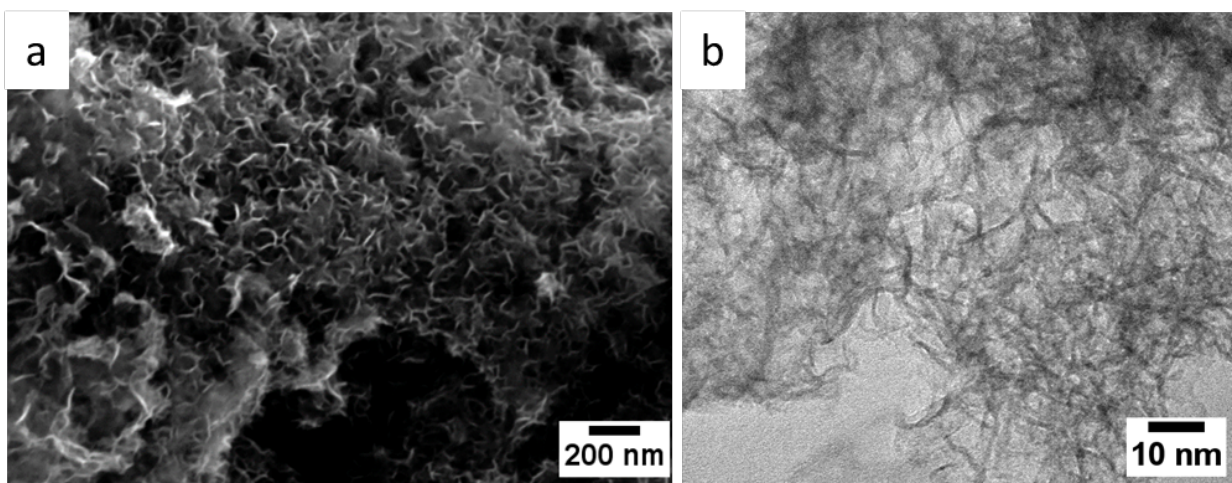


Fig. S4 (a) SEM and (b) TEM images of Ni_xB nanosheets.

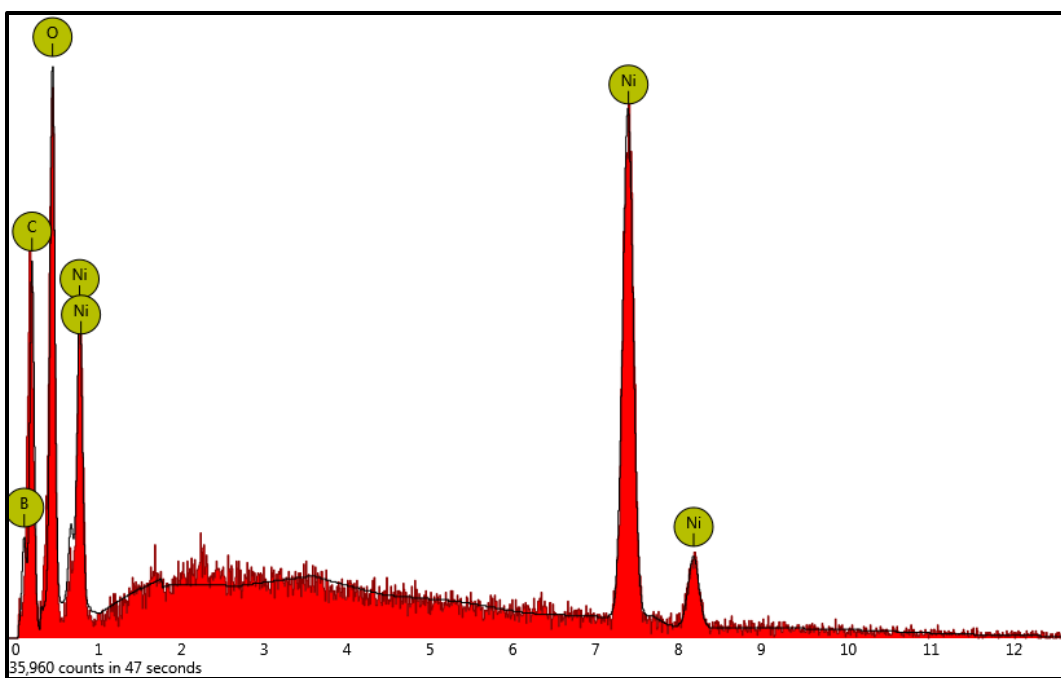


Fig. S5 EDS spectrum of $\text{Ni}_x\text{B}/\text{f-MWCNT}$.

Table S1 Elemental compositions (at. %) of f-MWCNT, Ni_xB , and $\text{Ni}_x\text{B}/\text{f-MWCNT}$ determined by EDX^a, XPS^b, and ICP^c.

Materials	C	O	B	Ni
f-MWCNT ^b	77.7	22.3	—	—
$\text{Ni}_x\text{B}^{\text{b}}$	—	—	26.31	73.69
$\text{Ni}_x\text{B}/\text{f-MWCNT}^{\text{a}}$	61.87	15.31	5.82	17.01
$\text{Ni}_x\text{B}/\text{f-MWCNT}^{\text{b}}$	47.10	20.02	8.13	24.75
$\text{Ni}_x\text{B}/\text{f-MWCNT}^{\text{c}}$	—	—	25.8	74.2

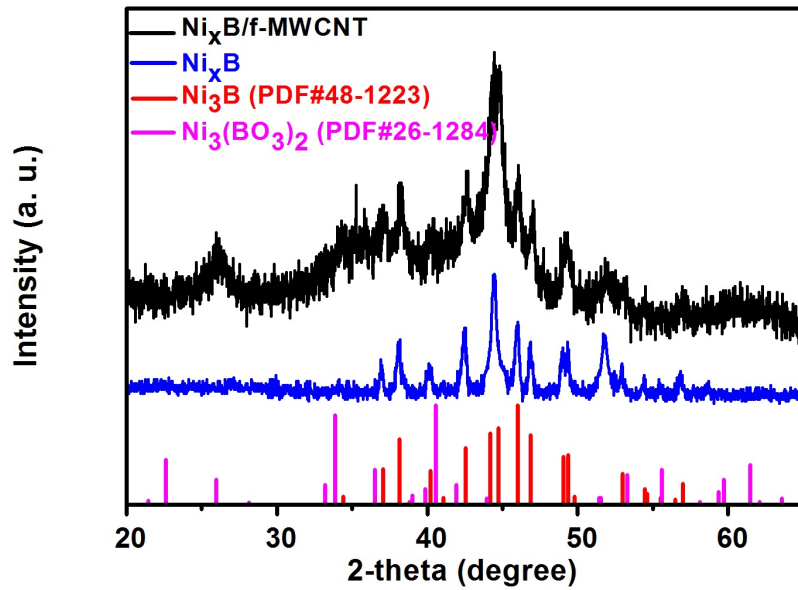


Fig. S6 XRD patterns of $\text{Ni}_x\text{B}/\text{f-MWCNT}$ and Ni_xB . The reference XRD peaks of Ni_3B (red vertical lines, JCPDS No. 48-1223) and $\text{Ni}_3(\text{BO}_3)_2$ (pink vertical lines, JCPDS No. 26-1284).

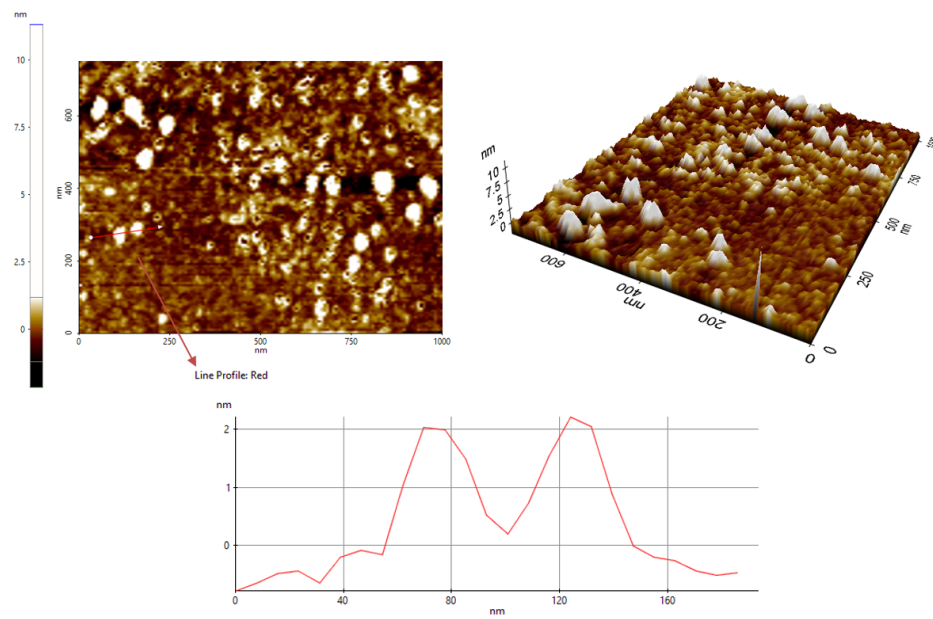


Figure S7 AFM images of $\text{Ni}_x\text{B}/\text{f-MWCNT}$ in 2D and 3D projection, recorded in the tapping mode, and the corresponding height profile.

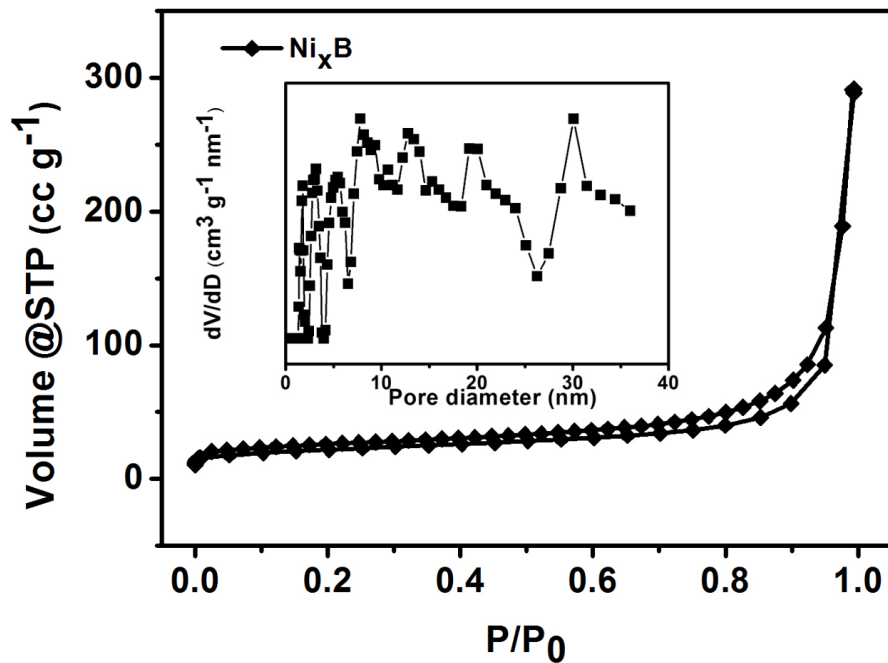


Fig. S8 Nitrogen adsorption-desorption isotherms of Ni_xB . The inset shows the pore size distribution of Ni_xB .

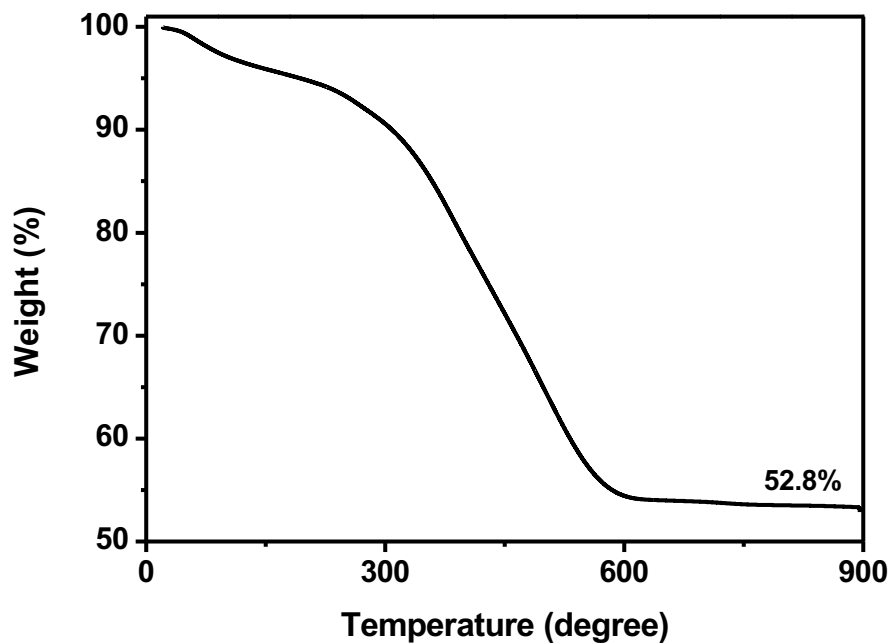


Fig. S9 TGA profile of $\text{Ni}_x\text{B}/\text{f-MWCNT}$.

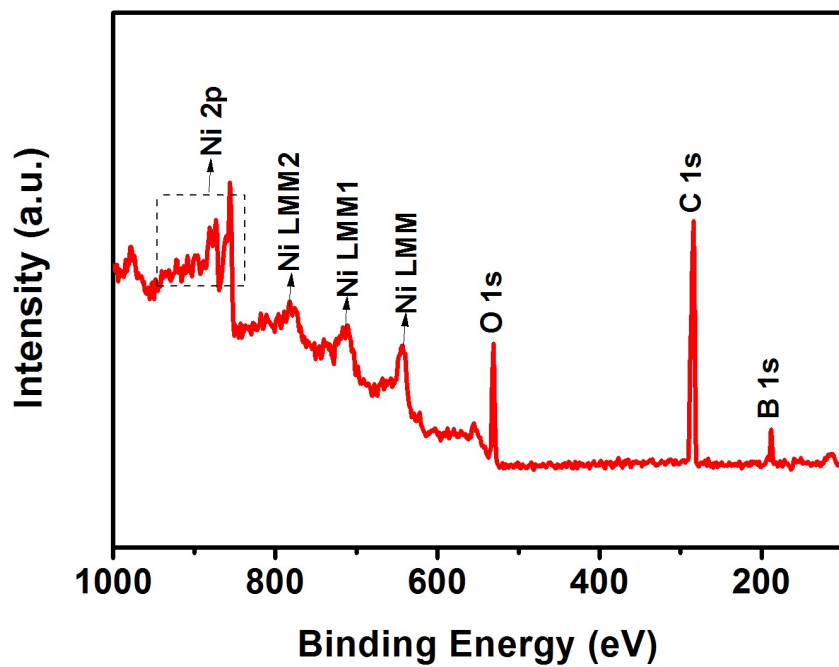


Fig. S10 XPS survey scan of $\text{Ni}_x\text{B}/\text{f-MWCNT}$.

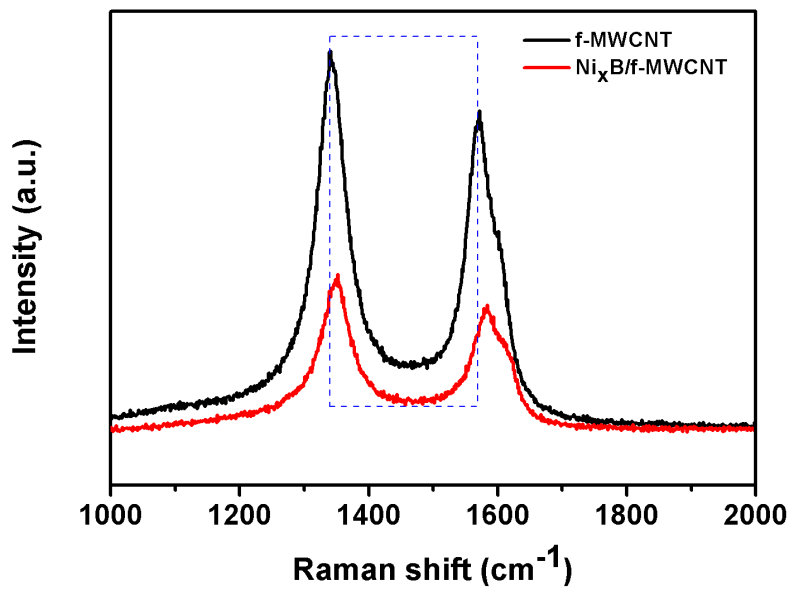


Fig. S11 Raman spectra of $\text{Ni}_x\text{B}/\text{f-MWCNT}$ and f-MWCNT.

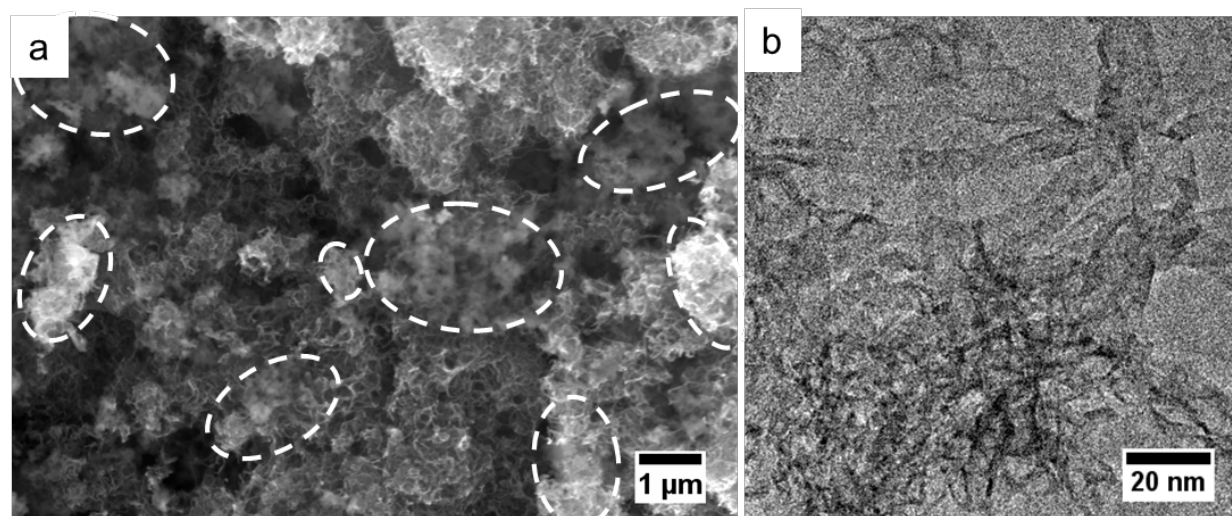


Fig. S12 (a) SEM and (b) TEM images of the physical mixture Ni_xB and f-MWCNT ($\text{Ni}_x\text{B}+\text{f-MWCNT}$). The areas circled by dashed lines show aggregated Ni_xB particles.

Table S2 Comparison of OER activity of recently reported nickel-based or metal-boride based electrocatalysts. (Note that the support material used in all examples given below.)

Catalyst	Loading (mg cm ⁻²)	Tafel slope (mV dec ⁻¹)	η_{10} (mV)	TOF (s ⁻¹)	Ref.
Ni_xB/f-MWCNT	0.2	46.3	286	0.058	<i>This work</i>
Ni_xB nanosheets	0.2	107.1	375	0.0432	<i>This work</i>
IrO₂ (reference)	0.2	71.2	338	—	<i>This work</i>
Pc-Ni-B@NB	0.3	52	302	0.026 0.052	<i>Angew. Chem. Int. Ed.</i> 2017 , <i>56</i> , 6572
Ni _x B-300	0.21	N/A	380	0.048	<i>Adv. Energy Mater.</i> 2017 , <i>7</i> , 1700381
Co ₂ B-500	0.21	45	380	—	<i>Adv. Energy Mater.</i> 2016 , <i>6</i> , 1502313
CoB NS/G	0.285	53	290	—	<i>Angew. Chem. Int. Ed.</i> 2016 , <i>55</i> , 2488
FeB ₂	0.2	52.4	296	—	<i>Adv. Energy Mater.</i> 2017 , <i>7</i> , 1700513
Ni ₃ B-rGO	0.2	88.4	290	—	<i>Electrochim. Commun.</i> 2018 , <i>86</i> , 121
Ni-Fe-B/rGO	0.2	58	265	—	<i>J. Solid State Chem.</i> 2018 , <i>265</i> , 13.
Co-Mo-B	2.1	150	320	—	<i>Electrochimica Acta.</i> 2017 , <i>232</i> , 64
Co-Ni-B@NF	—	131	313	—	<i>J. Mater. Chem. A</i> , 2017 , <i>5</i> , 12379.
NiO	0.14	65	365	—	<i>Energy Environ. Sci.</i> 2015 , <i>8</i> , 2347
Ni ₂ P	0.14	47	290	—	<i>Energy Environ. Sci.</i> 2015 , <i>8</i> , 2347
Ni-P	0.2	64	300	—	<i>Energy Environ. Sci.</i> 2016 , <i>9</i> , 1246
NiPS ₃	0.2	80	350	—	<i>ACS Catal.</i> 2017 , <i>7</i> , 229
NiPS ₃ -G-1:1	0.2	42.6	294	0.0564	<i>ACS Nano</i> 2018 , <i>12</i> , 5297
Ni _{0.6} Co _{1.4} (OH) ₂	0.35	80	300	—	<i>Adv. Funct. Mater.</i> 2018 , <i>28</i> , 1706008
Ni(OH) ₂	0.2	42	331	0.0361	<i>J. Am. Chem. Soc.</i> 2014 , <i>136</i> , 7077
Ni ₃ Se ₂	0.217	79.5	310	0.044	<i>Energy Environ. Sci.</i> 2016 , <i>9</i> , 1771
NGO/Ni ₇ S ₆	0.21	45.4	380	—	<i>Adv. Funct. Mater.</i> 2017 , <i>27</i> , 1700451

† N/A: not available.

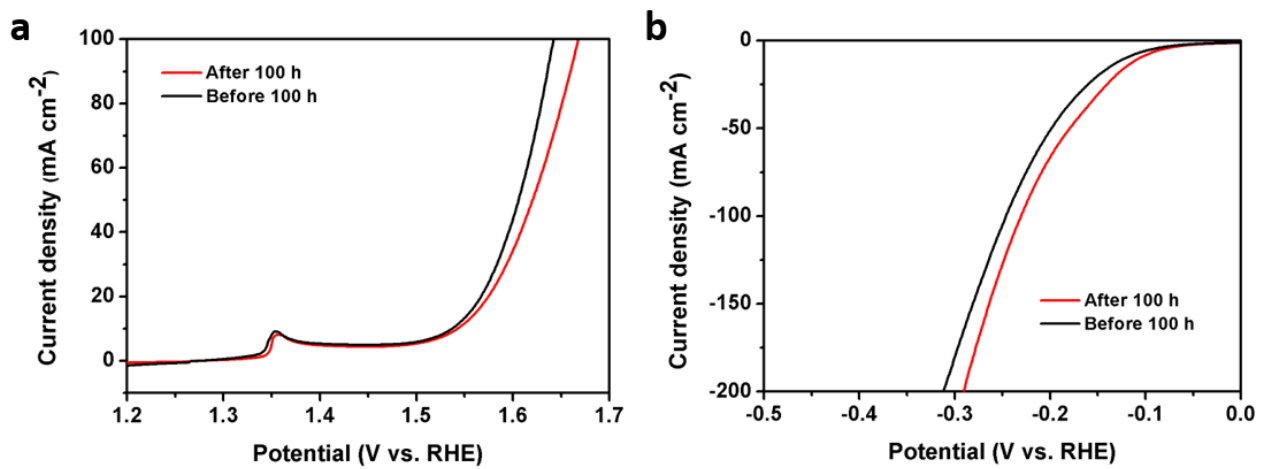


Fig. S13 Linear sweep voltammograms (LSVs) of $\text{Ni}_x\text{B}/\text{f-MWCNT}$ in 1.0 M KOH before and after Chronopotentiometry operation for 100 h under the current density of 20 mA cm^{-2} . a) OER, and b) HER.

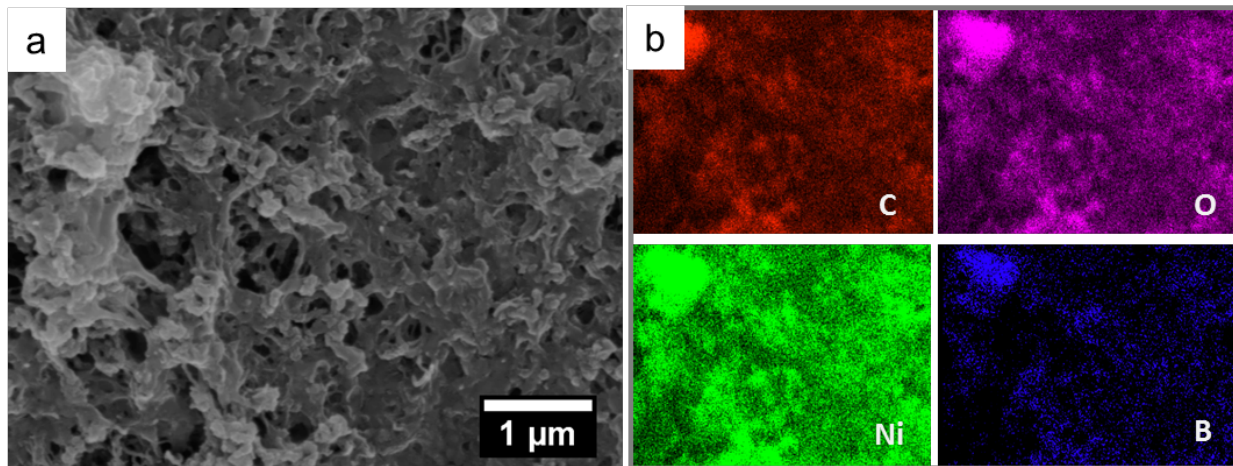


Fig. S14 Characterization of $\text{Ni}_x\text{B}/\text{f-MWCNT}$ after the 100-hour OER test in 1 M KOH electrolyte under the current density of 20 mA cm^{-2} . (a) SEM image and (b) the corresponding EDX elemental mappings of C, O, Ni, and B.

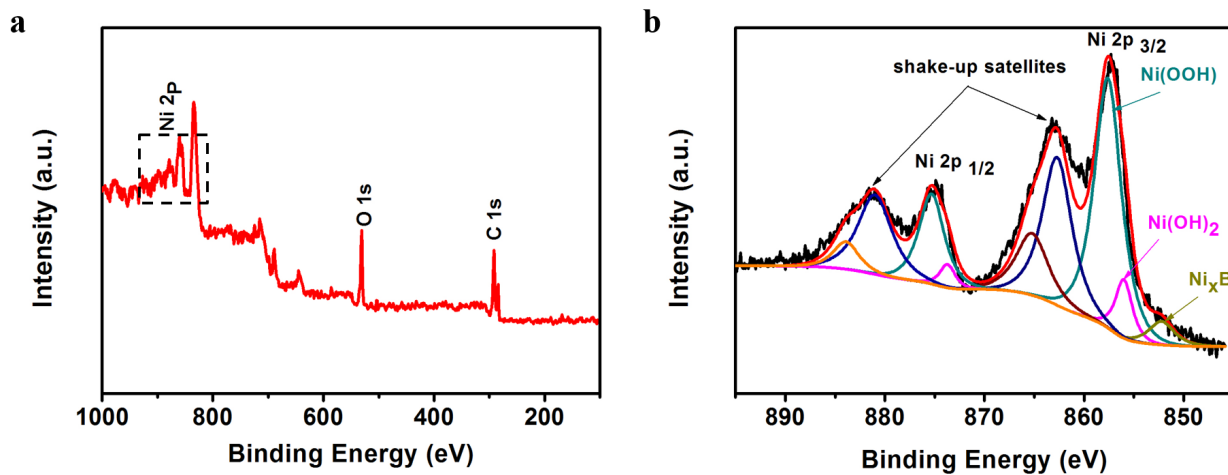


Fig. S15 (a) XPS survey spectrum of $\text{Ni}_x\text{B}/\text{f-MWCNT}$ after the 100-hour OER test in 1 M KOH electrolyte under the current density of 20 mA cm^{-2} , and (b) the corresponding core-level XPS spectra near the region of Ni2p.

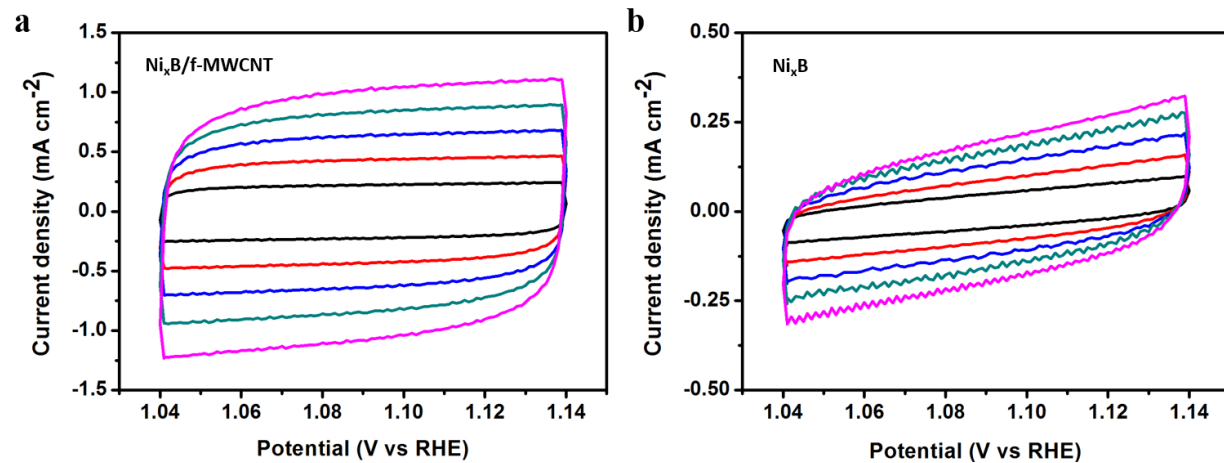


Fig. S16 Cyclic voltammogram (CV) curves of (a) $\text{Ni}_x\text{B}/\text{f-MWCNT}$ and (b) Ni_xB recorded in a non-Faradic region in 1 M KOH at different scan rates of 20, 40, 60, 80, and 100 mV s⁻¹.

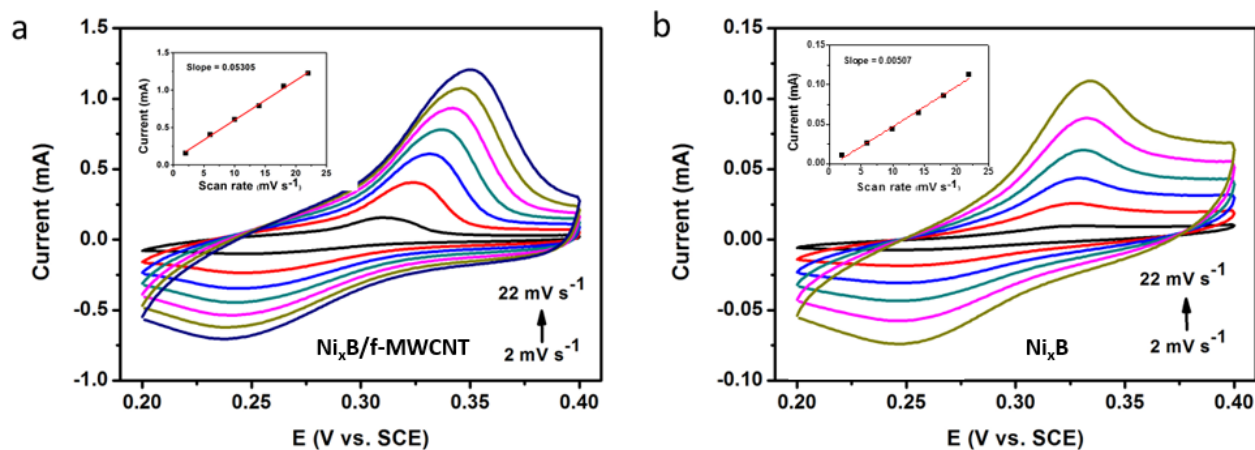


Fig. S17 CV curves of (a) $\text{Ni}_x\text{B}/\text{f-MWCNT}$ and (b) Ni_xB at the different scan rates from 2 to 22 mV s^{-1} in 1 M KOH electrolyte. The inset figures show the corresponding plots of the oxidation peak current *vs.* the scan rate extracted from (a) and (b), respectively.

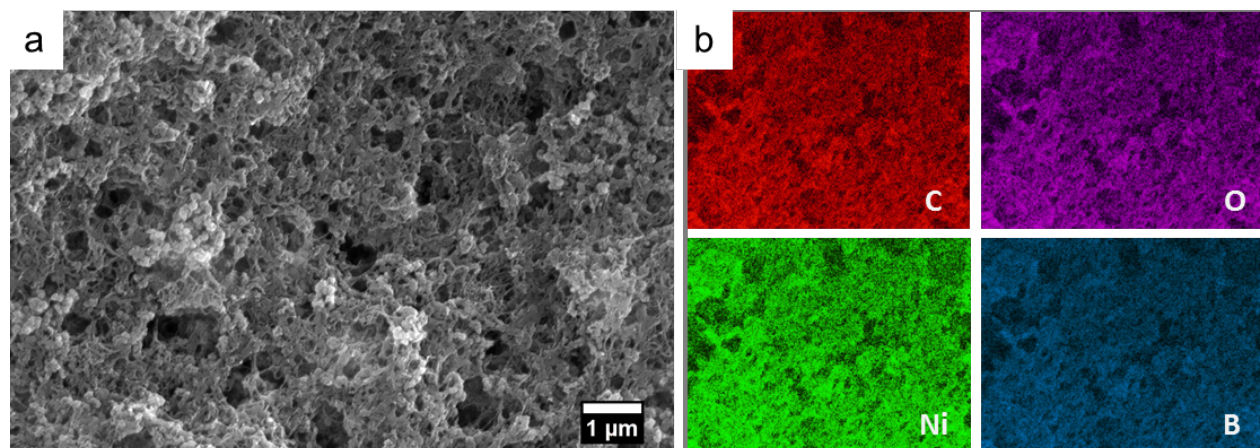


Fig. S18 Characterization of $\text{Ni}_x\text{B}/\text{f-MWCNT}$ after the 100-hour HER test in 1 M KOH electrolyte under the current density of 20 mA cm^{-2} . (a) SEM image and (b) the corresponding EDX elemental mappings of C, O, Ni, and B.

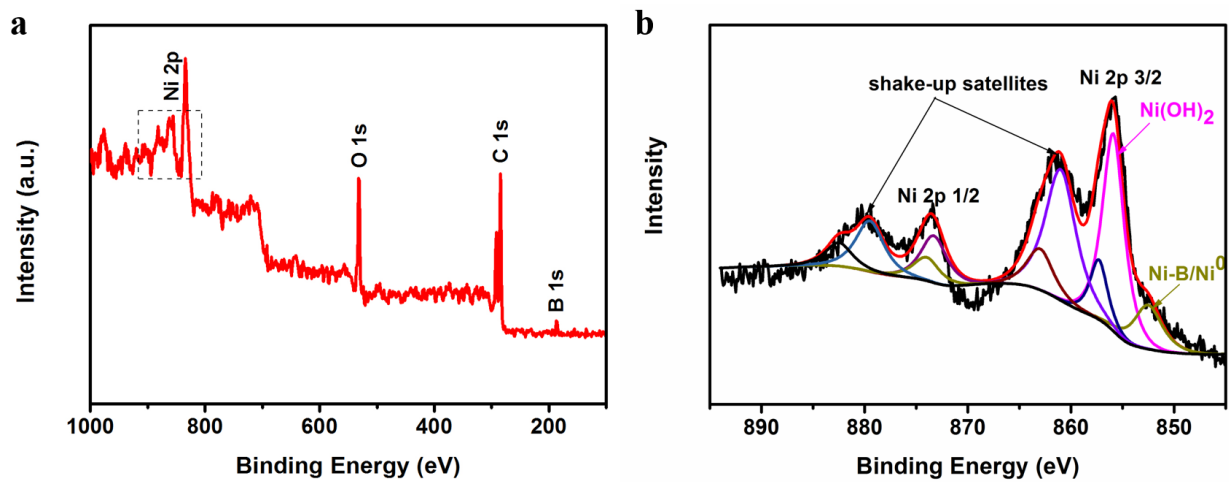


Fig. S19 (a) XPS survey spectrum of $\text{Ni}_x\text{B}/\text{f-MWCNT}$ after the 100-hour HER test in H_2 -saturated 1 M KOH electrolyte under the current density of 20 mA cm^{-2} , and (b) the corresponding core-level XPS spectra near the region of Ni2p.

Table S3. The HER performance of recently reported nickel- or TMB-based electrocatalysts.

Catalyst	Support	Loading (mg cm ⁻²)	Tafel slope (mV dec ⁻¹)	η_{10} (mV)	Ref.
Ni_xB/f-MWCNT	Glassy carbon	0.2	70.4	116	<i>This work</i>
Ni_xB nanosheets	S/A	0.2	152.1	277	<i>This work</i>
Ni_xB+f-MWCNT	S/A	0.2	103.9	209	<i>This work</i>
Pt/C (reference)	S/A	0.2	57.2	62	<i>This work</i>
Co ₂ B-500/NG	S/A	0.21	92.4	127	<i>Adv. Energy Mater.</i> 2016 , 6, 1502313
FeB ₂	S/A	0.2	87.5	61	<i>Adv. Energy Mater.</i> 2017 , 7, 1700513
NiO/Ni-CNT	S/A	0.28	82	<100	<i>Nat. Commun.</i> 2014 , 5, 4695
NiO nanorods	S/A	0.2	100	~110	<i>Nano Energy.</i> 2018 , 43, 103
1TMoS ₂ /Ni ^{2+δ} O _δ (OH) _{2-δ}	S/A	0.4	105	185	<i>Adv. Sci.</i> 2018 , 5, 1700644
MoC _x	S/A	0.8	59	151	<i>Nat. Commun.</i> 2015 , 6, 6512
Mo _x C-Ni@NCV	S/A	1.1	93	126	<i>J. Am. Chem. Soc.</i> 2015 , 137, 15753
Ni ₂ P	S/A	1.8	—	220	<i>Energy Environ. Sci.</i> 2015 , 8, 2347
Ni ₂ P	S/A	1	—	~180	<i>J. Am. Chem. Soc.</i> 2013 , 135, 9267
CoP	Carbon cloth	0.92	129	209	<i>J. Am. Chem. Soc.</i> 2014 , 136, 7587
NiCo ₂ S ₄	Nickel foam	—	58.9	210	<i>Adv. Funct. Mater.</i> 2016 , 26, 4661
N-doped Ni ₃ S ₂	S/A	0.6	113	155	<i>Adv. Energy Mater.</i> 2018 , 8, 1703538
NF-NiS ₂	S/A	—	63	122	<i>Nano Energy.</i> 2017 , 41, 148
Ni/NiS	S/A	—	123.3	230	<i>Adv. Funct. Mater.</i> 2016 , 26, 3314
o-CoSe ₂ P	o-CoSe ₂ P	1.02	69	104	<i>Nat. Commun.</i> 2018 , 9, 2533
NiSe/NF	Nickel foam	—	120	96	<i>Angew. Chem. Int. Ed.</i> 2015 , 54, 9351

† S/A: same as above.

Table S4. Comparison of the bifunctional water splitting activity of the Ni_xB/f-MWCNT catalyst with other recently reported bifunctional electrocatalysts in 1 M alkaline electrolytes.

Anode	Cathode	Loading (mg cm ⁻²)	η_{10} (mV)	Ref.
Ni _x B/f-MWCNT	Ni _x B/f-MWCNT	1.0	1.60	<i>This work</i>
IrO ₂ (reference)	Pt/C (reference)	1.0	1.62	<i>This work</i>
Ni/NiP	Ni/NiP	10.58	1.61	<i>Adv. Funct. Mater.</i> 2016 , <i>26</i> , 3314
Ni ₂ P	Ni ₂ P	5	1.63	<i>Energy Environ. Sci.</i> 2015 , <i>8</i> , 2347
NiCo ₂ P ₂ /G NSs	NiCo ₂ P ₂ /G NSs	0.31	161	<i>Nano Energy.</i> 2018 , <i>48</i> , 284
Ni ₁₁ (HPO ₃) ₈ (OH) ₆	Ni ₁₁ (HPO ₃) ₈ (OH) ₆	3	1.65	<i>Energy Environ. Sci.</i> , 2018 , <i>11</i> , 1287
NiSe/NF	NiSe/NF	2.8	1.63	<i>Angew. Chem. Int. Ed.</i> 2015 , <i>54</i> , 9351
NiCo ₂ O ₄	Ni _{0.33} Co _{0.67} S ₂	0.3	1.72	<i>Adv. Energy Mater.</i> 2015 , <i>5</i> , 1402031
Co _{0.85} Se/NiFe-LDH	Co _{0.85} Se/NiFe-LDH	4	1.66	<i>Energy Environ. Sci.</i> 2016 , <i>9</i> , 478
BSCF/NF	BSCF/NF	0.387	1.72	<i>Sci. Adv.</i> 2017 , <i>3</i> , e1603206
Ni ₅ P ₄ films/Ni	Ni ₅ P ₄ films/Ni	3.5	~1.68	<i>Angew. Chem. Int. Ed.</i> 2015 , <i>127</i> , 12538
SNCF-NR	SNCF-NR	3	1.68	<i>Adv. Energy Mater.</i> 2017 , <i>7</i> , 1602122
Fe-doped CoP	Fe-doped CoP	1.03	1.60	<i>Adv. Mater.</i> 2017 , <i>29</i> , 1602441
NiCo ₂ S ₄ /NF	NiCo ₂ S ₄ /NF	6.5	1.61	<i>Adv. Mater. Interf.</i> 2018 , <i>5</i> , 1701396
CP/CTs/Co-S	CP/CTs/Co-S	0.32	1.743	<i>ACS Nano.</i> 2016 , <i>10</i> , 2342
NiFeO _x /CFP	NiFeO _x /CFP	1.6	~1.61	<i>Nat. Commun.</i> 2015 , <i>6</i> , 8261
NiFe LDH/NF	NiFe LDH/NF	–	1.70	<i>Science</i> 2014 , <i>345</i> , 1593
Ni ₃ FeN/r-GO	Ni ₃ FeN/r-GO	0.5	1.60	<i>ACS Nano</i> 2018 , <i>12</i> , 245

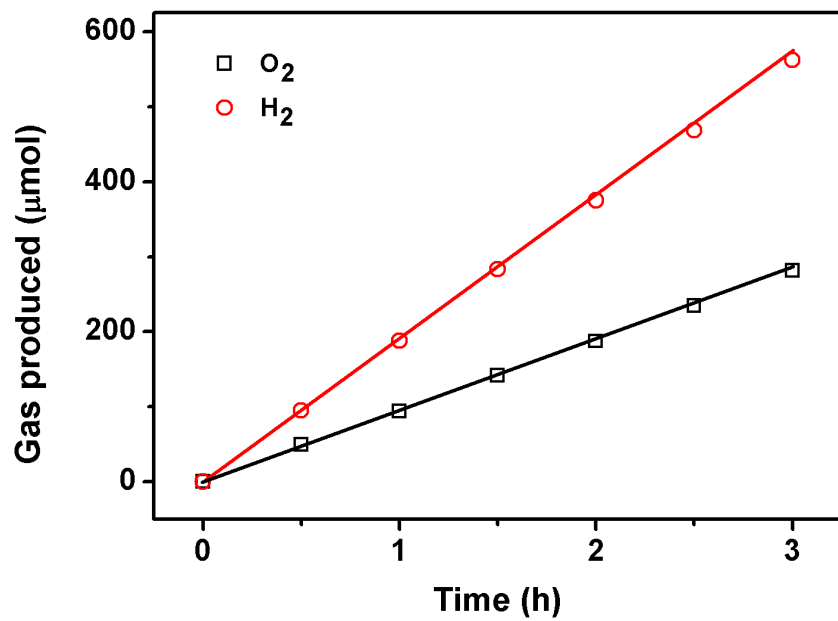


Fig. S20. The amount of gas theoretically calculated and experimentally measured vs. time for OER and HER vs. time for Ni_xB/f-MWCNT.